ORIGINAL ARTICLE

Liver Histopathological Evaluation after Injection of CIDR1α-PfEMP1 Protein Recombinant in Rats

Rosita Dewi[1], Erma Sulistyaningsih[2], Teguh Prasetyo[3], Sheilla Rachmania[1], Irawan Fajar Kusuma[4]

[1] Department of Histology, Faculty of Medicine, University of Jember, Jember, Indonesia,
[2] Department of Parasitology, Faculty of Medicine, University of Jember, Jember, Indonesia,
[3] Undergraduate Medical Science Program, Faculty of Medicine, University of Jember, Jember, Indonesia,
[4] Department of Public Health, Faculty of Medicine, University of Jember, Jember, Indonesia

ABSTRACT

Introduction: Malaria vaccines are continuously developed to control malaria and prevent morbidity and mortality. The cysteine-rich interdomain region 1α of *Plasmodium falciparum erythrocyte membrane protein 1* (CIDR1α-PfEMP1) is a vital antigenic protein in malaria pathogenesis. This protein induces an increase of IgM, IgG, and CD4+. Preclinical safety evaluation is the next critical stage in candidate vaccine testing, including organ safety testing. Foreign substance accumulation in the liver potentially causes liver inflammation and damages its structure. Objectives: This study aimed to evaluate liver histopathology after injection of CIDR1α-PfEMP1 recombinant protein in rats. **Methods:** This study aimed to assess the liver structure after injection of CIDR1α-PfEMP1 recombinant protein in rats. We used 12 rats divided into two groups, i.e., the treatment group was injected with 150μg CIDR1α-PfEMP1, and the control group was injected with 0.9% NaCl solution on days 0, 21, and 42. Necropsy was performed on day 56, and liver histopathological slides were prepared and stained using hematoxylin-eosin. The liver histopathological evaluation included Kupffer cell count and hepatocyte damage scoring using Manja Roenigk criteria. **Results:** The average number of Kupffer cells in the treatment and the control group were 14.25±4.6 and 14.12±3.43 per visual field, while the average score of hepatocyte damage score in the treatment and control group were 101±0.55 and 100.62±0.41, respectively. The Mann-Whitney analysis for both indicators showed no significant difference between the control and treatment groups ($p>0.05$). **Conclusion:** There is no inflammation and hepatocyte damage after injection of CIDR1α-PfEMP1 recombinant protein in rats.
Malaysian Journal of Medicine and Health Sciences (2026) 22(SUPP7): 87-93. doi:10.47836/mjmhs.22.s7.14

Keywords: CIDR1α, PfEMP1, Malaria, Liver, Hepatocyte

Corresponding Author:
Erma Sulistyaningsih, PhD
Email: sulistyaningsih.fk@unej.ac.id
Tel: +62-331-337877.

INTRODUCTION

Malaria is one of the global health problems and can be found in 85 countries worldwide. In Indonesia, although a 5% decrease in the number of cases has been reported, the total number of malaria cases still reaches 1,040,000 (1). The majority of malaria is caused by *Plasmodium falciparum* (*P. falciparum*), with a high probability of severe clinical symptoms and even death (2). Controlling malaria is part of achieving the Sustainable Development Goals, i.e., reducing the incidence and mortality due to malaria by at least 90% and eliminating malaria in 35 countries by 2030 (3, 4). World Health Organization (WHO) recommends several approaches to control malaria, including vaccine development.

However, developing a potential malaria vaccine is complicated due to the intricacy of antigenic protein expressed in the *P. falciparum* life cycle. One approved malaria vaccine is RTS,S, the name comes from Repeat ('R') and T-cell epitope ('T') of the pre-erythrocytic circum-sporozoite protein (CSP) of the *P. falciparum* parasite with a surface antigen ('S') of the hepatitis B virus and mixed with additional hepatitis B surface antigen (HBsAg) ('S'), the vaccine using the circum-sporozoite protein (CSP) as a target protein. This vaccine is currently advised for children in the high *P. falciparum* transmission area. Nevertheless, the effectiveness of vaccination fades after 18 months and only reaches 55% after 12 months out (5, 6). Hence, the exploration of the antigen proteins that have the potential to become vaccine candidates continues to be carried out.

One notable protein for malaria vaccine candidate is *Plasmodium falciparum* erythrocyte membrane protein-1 (PfEMP1), an adhesion protein that has an essential role in the pathogenesis of severe malaria. The protein is encoded by the var gene and expressed during the erythrocytic phase and further deposited on the surface of *P. falciparum*-infected erythrocytes in the knob protrusion area (7). PfEMP1 has two major

domains, namely the Duffy binding-like (DBL) domain and the Cysteine-rich interdomain region (CIDR). The CIDR domain, flanked by two DBL domains, can be found regularly in the var gene's head structure (7, 8).

The CIDR1α-PfEMP1 has binding capacities to endothelial protein C receptor (EPCR) and Cluster of Differentiation (CD)36 receptors, which play pivotal roles in severe malaria pathogenesis (9). Protein C activation regulates coagulation, blood vessel permeability, and blood vessel inflammation, resulting in PfEMP1 binding to EPCR, which subsequently causes inflammation and coagulation of cerebral blood vessels. A former study described that patients with complicated malaria had a larger proportion of the var gene, which encodes for CIDR1α bound to EPCR by a median percentage of 54.1%, compared to patients with uncomplicated malaria, a median percentage of 7.4% (8). Therefore, the development of malaria vaccine based on the CIDR1α-PfEMP1 is intended to prevent the severe clinical symptoms of malaria due to *P. falciparum* infection, as the role of the CIDR1α-PfEMP1 in the pathology of malaria.

As a protein target for the development of a subunit-based malaria vaccine, we explored CIDR1α-PfEMP1. A previous study in rats displayed that 150 µg CIDR1α-PfEMP1 injection raised IgM level following primary injection, IgG level after primary, secondary-1, and secondary-2 injections, and CD4+ level after secondary-2 injection, (10, 11) antibodies are expected to obstruct the binding of the CIDR1α domain to CD36 and EPCR receptors. Another study also demonstrated that DBL2β-PfEMP1-induced antibodies blocked cytoadherence and interfered with rosette formation, reducing the probability of severe malaria by 37% (12).

The next important stage in candidate vaccine testing is preclinical safety evaluation in vital organs, including the liver, as the main metabolic organ, putting it at high risk of experiencing changes in function and structure (13, 14). Liver injury due to exposure to foreign substances can be evaluated microscopically by observing the inflammatory cell infiltration, liver degeneration, and necrosis (14, 15). A further fascinating microscopical evaluation is the Kupffer cells (KCs). Those cells are non-parenchymal liver cells located in the sinusoidal lining of the liver, making up 15% of the total liver cells (16). They are the most abundant macrophage in the body and contribute most to the pathogenesis of liver injury and liver homeostasis (17). Toxic agents-induced liver injury releases various signaling molecules activating KCs that can cause inflammation in the liver by releasing various inflammatory mediators and chemokines, then generating reactive oxygen species (ROS) production (18–20).

A prior study stated that activated KCs were mostly found in rats administered diazinon at a dose of 40 mg/kgBW for 7 days (21), while another study using the Manja Roenigk criteria demonstrated the increased liver cells damage score due to diazinon (22). Currently, no preclinical safety studies involving the liver have been carried out in relation to the CIDR protein as a potential malaria vaccine. Therefore, this study aimed to evaluate liver histopathology after injection of CIDR1α-PfEMP1 recombinant protein in rats.

MATERIALS AND METHODS

This study was performed at The Laboratory of Biotechnology and Biology Molecular, Faculty of Medicine, University of Jember, from December 2022 to May 2023 and has received ethical approval from The Ethical Committee of the Faculty of Medicine, University of Jember with the accession nr. 1826/H25.1.11/KE/2023. The former study has successfully cloned the CIDR1α-PfEMP1 target gene. The CIDR1α-PfEMP1 recombinant was produced in Escherichia coli BL-21(DE3) cells (23, 24). The production and purification of the CIDR1α-PfEMP1 were carried out as a previous study. The protein concentration was measured using the Bradford protein assay (HiMedia Laboratories, Maharashtra, India, with catalog number ML106-500 ML) at 595 nm. It was 27 kDa protein (10). The purified protein was calculated by entering the absorbance value based on the formula: y=0.0078x-0.0703 (R2=0,9962). The concentration of purified protein that we obtained was in the range of 0.8-1 µg/µL.

The experimental animals

The number of Wistar rats (*Rattus norvegicus*) was calculated using the resource equation formula (25). We obtained the E-value within the expected range (14). Nevertheless, to apply the principle of reduction, we used 4 rats for the control group. This reduction was associated with practical, ethical, and research efficiency considerations (26). Hence, we used 12 male Wistar rats, 2-3 months old, weighing 150-250 grams, and were divided into two groups, 4 rats for the control group and 8 rats for the treatment group. Rat acclimatization was carried out for 14 days. Rats were kept in plastic boxes (40 cm x 30 cm x 13 cm), completed with food containers and plastic bottles, two rats per box.

The injection of the CIDR1α-PfEMP1 recombinant protein

Each rat in the treatment group was injected with 150 µg purified CIDR1α-PfEMP1 protein, and the rat in the control group was injected with 0.9% Natrium Chloride (NaCl) subcutaneously on day 0 for primary injection, on day 21 for secondary-1 injection, and on day 42 for secondary 2 injection (27–29). This study used only a dose of 150 µg purified CIDR1α-PfEMP1 protein based on the standard immunization of rats using protein (27) and previous study with a similar design (29). Subcutaneous administration was chosen to increase the probability

of contact with Langerhans cells, which act as antigen-presenting cells, and to induce an optimal immune response (30). Furthermore, as the protein has more than 20 kDa molecular weight, subcutaneous injection could be transported through blood vessel capillaries and requires transport through the lymphatic system, which is accessed through subcutaneous injection (31).

The CIDR1α-PfEMP1 recombinant protein was combined with Complete Freund's Adjuvant (Santa Cruz, cat number sc-3727) at a 1:1 ratio for the initial injection and Incomplete Freund's Adjuvant (Santa Cruz, cat number sc-24019) for the secondary injection to guarantee a steady release of antigens, which is necessary to elicit a strong and long-lasting immune response. In order to draw macrophages and other immune cells to the injection site, the Complete Freund's Adjuvant (CFA), which contains heat-killed Mycobacterium tuberculosis, was used for the first injection. It will improve the immune response by maximizing the recombinant protein's exposure to the antigen-presenting cell. Without the mycobacteria, the Incomplete Freund's Adjuvant (IFA) contains the same chemical as CFA and was used for booster immunization without any of the side effects of CFA (32, 33).

The necropsy and liver histopathological observation
On day 56, a necropsy was performed on the experimental animals under anesthesia using ketamine and xylazine with a dose of 91 mg/kg ketamine and 9.1 mg/kg xylazine (34). The right lobe of the liver was taken with a transversal cut (35). Histopathological observation of the liver was carried out using an Olympus CX21LED microscope and photographed using an Optilab 3.0 camera.

Examination on Kupffer cells (KCs) was performed only for the activated KC. The activated KCs can be distinguished from inactivated KCs by their size, shape, and location. The activated KCs exhibited extended cytoplasmic processes and open-face type cells located along the sinusoid and were seen interacting with endothelial cells, collagen fibers, and other KCs (36). Observation of activated KCs was carried out in 10 visual fields of the microscope in 400X magnification; each visual field was documented using FIJI ImageJ software, and the number of activated was counted. The number of activated KCs was categorized as follows: (1) grade 0 if the KCs number <20; (2) grade 1 if the KCs number 20-35; (3) grade 2 if the KCs number 35-50; (4) grade 3 if the KCs number >50 (18).

Further histopathological examination was hepatocyte damage using the Manja Roenigk criteria. The assessment was carried out using a microscope with 400X magnification on 5 visual fields in zone-3 of the liver around the central vein, with 20 hepatocytes per visual field. So, a total of 100 cells were chosen (37). The hepatocyte score was classified into 4 grades: (1) grade 1 for normal hepatocytes with the characteristics of polygonal cells, homogeneous red cytoplasm, and cell membranes with clear boundaries; (2) grade 2 for parenchymal degeneration with the characteristics of swollen cells, cloudy cytoplasm, and the appearance of granules in the cytoplasm; (3) grade 3 for hydropic degeneration with the characteristics of swollen cells and pale cytoplasm with vacuolization; and (4) grade 4 for necrosis hepatocyte with the characteristics of shrunken cell nuclei with a darker color (pyknotic), destroyed cell nuclei to form fragments (karyorrhexis), or chromatin and dissolved cell nuclei (karyolysis) (38).

The examination was performed by two observers, and the Cronbach alpha test was measured to ensure reliability (39–41). The Cronbach alpha, which is considered as an acceptable value, is 0-1, yet α>0.7 is a recommended value in most studies (42).

The statistical analysis
The number of activated KCs and liver histopathology damage scores in the control and treatment groups were presented descriptively based on the examiner's calculations. And the different between the control and treatment groups were analyzed using the Mann-Whitney U statistical test.

RESULTS

The number of activated KCs
Qualitative observation of activated KCs showed amoeboid cytoplasm forming protrusions, open-face type, with varying sizes and shapes along the sinusoid, as presented in Figure 1. The range of activated KCs count per visual field of the control group was 10-19.5 (all categorized as grade 0) with an average of 14.12±3.43, and the treatment group was 7.5-20.5 (7 rats categorized as grade 0 and 1 rat categorized as grade 1) with an average of 14.25±4.6 (Table I).

The Cronbach alpha test showed a value of 0.994 (α >0.7), indicating its reliability. The Mann-Whitney test revealed a significance value of 0.48 (p>0.05), meaning no significant difference between the control and treatment groups.

The histopathological liver damage score
The majority of hepatocytes showed normal characteristics, which are polygonal in shape, homogeneous red cytoplasm, cell membranes with clear boundaries, and no enlargement, as presented in Figure 2. A small proportion of hepatocytes in the control and treatment groups showed parenchymal degeneration characteristics, which is a swollen, cloudy cytoplasm with granules—neither hydropic degeneration nor necrosis was found in either group. The range of total liver histopathology damage score of the control group was presented in Table II.

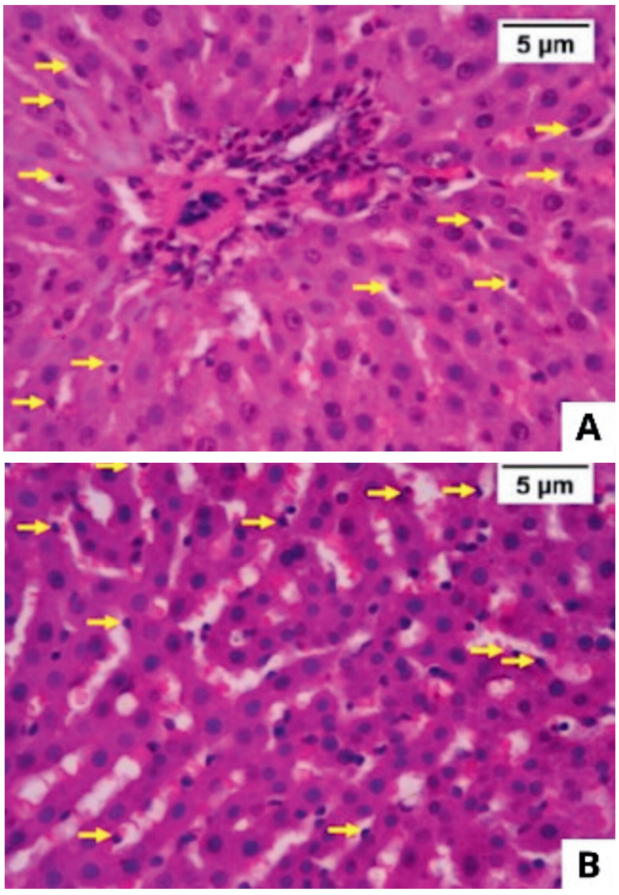

Figure 1: The structure of activated KCs in liver (400X magnification). It showed amoeboid cytoplasm, open-face type, along the sinusoid (yellow arrows). A: the control group; B: the treatment group.

Table I: The number of activated KCs

Groups		Activated KCs per field of view per rat *)	Grade	Activated KCs (visual field/ group) ± SD**)
Control	C1	14	0	14.12±3.43
	C2	19.5	0	
	C3	13	0	
	C4	10	0	
Treatment	T1	15.5	0	14.25±4.60
	T2	16.5	0	
	T3	7.5	0	
	T4	18.5	0	
	T5	10.5	0	
	T6	20.5	1	
	T7	8	0	
	T8	17	0	

*) The average number of activated KCs (Kupffer cells) per field of view per rat
**) The average number of activated KCs per field of view per group ± SD
KCs: Kupffer Cells
SD: Standard Deviation

The Cronbach alpha test for hepatocyte score resulted in a value of 0.766 (α >0.7), indicating that the data were reliable. The Mann-Whitney test showed a significance value of 0.52 (p>0.05), indicating no significant difference between the control and treatment groups.

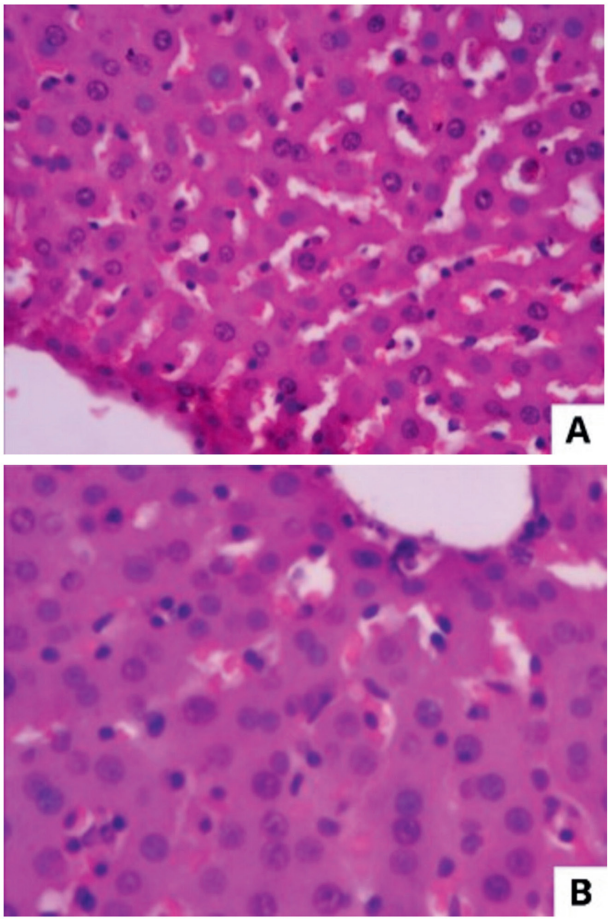

Figure 2: The histopathology of the liver showed normal hepatocytes which are polygonal in shape, homogeneous red cytoplasm, cell membranes with clear boundaries, and no enlargement. A: the control group; B: the treatment group.

Table II: The liver histopathology damage score based on Manja Roenigk criteria

Groups		Score per rat *)	Liver histopathology damage score per hepatocyte **)	Average of total liver histopathology damage score per group ± SD
Control	C1	100.5	1.00	100.62±0.41
	C2	101	1.01	
	C3	100	1.00	
	C4	101	1.01	
Treatment	T1	101	1.01	101.00**±0.55**
	T2	101.5	1.01	
	T3	101	1.01	
	T4	101	1.01	
	T5	101.5	1.00	
	T6	102	1.02	
	T7	100	1.00	
	T8	100	1.01	

*) The average of total liver histopathology damage score per rat
**) The average of total liver histopathology damage score per hepatocyte

DISCUSSION

The liver is an organ that has various complex and important functions for the body, including metabolism and detoxification (13, 14). Structural liver changes in a safety test can be observed through histopathological examination. The right lobe of the rat liver was the part of the liver taken to make histopathological slides. Anatomically, the right lobe has greater vascularization than the other lobes, namely the dorsal branch of the right lateral lobe (r. dorsalis lobi lateralis dextri), the intermediate branch of the right lateral lobe (r. intermedius lobi lateralis dextra), and the ventral branch of the right lateral lobe (ventralis lobi lateralis dextri) (35). Previous tests on the hepatotoxic property of a substance were carried out on the right lobe, such as observing liver cell damage due to malathion induction, which is a group of organophosphates (43). Another similar study was that sodium arsenide induction was able to cause more severe liver cell damage in the right lobe compared to the other lobes (44).

The number of activated KCs between the control and treatment groups did not differ significantly ($p>0.05$). This indicates that the recombinant protein does not increase the number of KCs, which is a marker of inflammation and oxidative stress in the liver. The KCs, non-parenchymal liver cells, are found along the liver's sinusoid and account for 80–90% of the tissue macrophages in the reticuloendothelial system and 15% of all liver cells (16). Being the most prevalent macrophage in the body, they play a major role in the etiology of liver injury and in maintaining hepatic homeostasis (17). As the first line of defense exposed to foreign substances, they eradicate and detoxify the invading foreign pathogens. Since IFN-γ binds to its receptor on macrophages, the signal transducers, activators of transcription 1 (STAT1), and interferon regulatory factors (IRF) will be activated, resulting in the KCs activation (19).

The number of activated KCs can be one of the parameters of inflammation in the liver, which occurs through the release of various inflammatory mediators and chemokines and then generating reactive oxygen species (ROS) production. Activated KCs existence is not only characterized by the high capacity to present antigen, strong expression and secretion of IRF-5, interleukin-23 (IL-23), and interleukin-12 (IL-12), but also much production of ROS as a defense against toxic agent. Therefore, the increase in ROS production is related to the increased number of activated KCs, which can cause oxidative stress conditions that lead to liver damage (19, 20). This explanation is supported by Owumi et al. (2014), who revealed that the depletion of KCs reduced cytokines releases and ROS production, consequently improving ethanol-induced liver damage (17).

Neither the number of activated KCs nor the histopathological liver damage score between the treatment and control groups was significantly different ($p>0.05$). The histopathological liver damage was observed on hepatocytes in zone 3 of the liver lobule around the central vein. Liver cells in zone 3 have different functions from other zones. They have the highest levels of cytochrome P-450 enzymes to metabolize various substances. This causes liver cells in zone 3 to be most strongly influenced by exposure to exogenous substances, so histopathological changes in liver cells are best observed in zone 3 (37). Qualitatively, parenchymal degeneration was found, but neither hydropic degeneration nor necrosis was found in either group, with an average score of 1.00-1.02 per hepatocyte.

Parenchymal degeneration is associated with ATP depletion due to exposure to foreign substances that result in failure of protein transport synthesized by ribosomes out of hepatocytes. The next level of damage is hydropic degeneration, which is also associated with ATP depletion, which pushes water and Na+ ions into the cell and K+ ions out of the cell. Cells are unable to eliminate water and cell organelles, so water accumulates in the cell (45, 46). According to the necrosis stages, pyknosis, karyorrhexis, and karyolysis are three stages of necrosis, respectively (47, 48). Necrosis is also associated with ATP depletion, which causes a compensating mechanism by increasing anaerobic glycolysis. This process causes a decrease in the amount of glycogen and an increase in lactic acid, which will cause changes in pH, which will then cause changes in the cell nucleus in the form of compaction of the nuclear chromatin, rupture of the cell nucleus, and fade of the cell nucleus (45, 46). Similar results from a prior study on circum-sporozoite protein (FMP013), a potential malaria vaccine, indicated that the substance was safe for animal use (49). Outside of malaria vaccine research, research conducted by Kandeil et al. (2021) on the safety test of the SARS-CoV-2 vaccine based on recombinant protein in hamsters stated that there were no significant histopathological changes observed in the liver (50).

However, further examination of liver functions through the level of liver enzymes, i.e., alanine transaminase (ALT), aspartate transaminase (AST), alkaline phosphatase (ALP), and bilirubin, is needed. Furthermore, the identification of liver inflammation or liver oxidative stress using immunohistochemistry methods and observing other microscopic liver structures, such as sinusoid congestion and portal tract inflammation, will be valuable to overcome considering the study limitations (18).

CONCLUSION

In conclusion, this study found no inflammation based on activated KCs counting and hepatocyte damage based

on the liver histopathology damage score after injection of CIDR1α-PfEMP1 recombinant protein in rats.

REFERENCES

1. Nazhid ARM, Wulandari S. Buletin APBN. Pus Anal Anggar Akuntabilitas Keuang Negara. 2023;8(23):3-6.
2. Bernabeu M, Smith JD. EPCR and malaria severity: the center of a perfect storm. Trends Parasitol. 2017;33(4):295-308. doi:10.1016/j.pt.2016.11.004
3. Moreno A, Joyner C. Malaria vaccine clinical trials: what's on the horizon. Curr Opin Immunol. 2015;35:98-106. doi:10.1016/j.coi.2015.06.007
4. World Health Organization. World malaria report 2022. Geneva: World Health Organization; 2022.
5. Zavala F. RTS,S: the first malaria vaccine. J Clin Invest. 2022;132(1):e156588. doi:10.1172/JCI156588
6. World Health Organization. World malaria report 2022. Geneva: World Health Organization; 2023.
7. Lee WC, Russell B, Rйnia L. Sticking for a cause: the falciparum malaria parasites cytoadherence paradigm. Front Immunol. 2019;10:1444. doi:10.3389/fimmu.2019.01444
8. Jespersen JS, Wang CW, Mkumbaye SI, Minja DT, Petersen B, Turner L, et al. *Plasmodium falciparum* var genes expressed in children with severe malaria encode CIDRα1 domains. EMBO Mol Med. 2016;8(8):839-50. doi:10.15252/emmm.201606188
9. Jensen AR, Adams Y, Hviid L. Cerebral *Plasmodium falciparum* malaria: the role of PfEMP1 in its pathogenesis and immunity, and PfEMP1-based vaccines to prevent it. Immunol Rev. 2020;293(1):230-52. doi:10.1111/imr.12807
10. Sulistyaningsih E, Wibisono R, Dewi R. Leukocyte and IgM responses to immunization with the CIDR1α-PfEMP1 recombinant protein in the Wistar rat. Trop Med Infect Dis. 2022;7(9):222. doi:10.3390/tropicalmed7090222
11. Istinaroh N, Sulistyaningsih E, Dewanti IDAR. IgG and CD4+ response post immunization with CIDR1α-PfEMP1 recombinant protein. J Kedokt Kesehat. 2024;18(2).
12. Tessema SK, Nakajima R, Jasinskas A, Monk SL, Doolan DL, Mueller I, et al. Protective immunity against severe malaria is associated with antibodies to a conserved repertoire of PfEMP1 variants. bioRxiv. 2018:1-27.
13. Holz LE, Fernandez-Ruiz D, Heath WR. Protective immunity to liver-stage malaria. Clin Transl Immunology. 2016;5(10):e105. doi:10.1038/cti.2016.68
14. Taek A, Ndaong N, Gaina C. Gambaran histopatologi hepar tikus putih (Rattus norvegicus) jantan pasca pemberian ekstrak infusa buah pare (Momordica charantia L.) lokal NTT. J Vet Nusant. 2020;3(2):89-96.
15. Ayun AQ, Faridah DN, Yuliana ND, Andriyanto A. Pengujian toksisitas akut LD50 infusa benalu teh (Scurrula sp.) dengan menggunakan mencit (Mus musculus). Acta Vet Indones. 2021;9(1):53-63.
16. Dixon LJ, Barnes M, Tang H, Pritchard MT, Nagy LE. Kupffer cells in the liver. Compr Physiol. 2013;3(2):785-97. doi:10.1002/cphy.c120026
17. Owumi SE, Corthals SM, Uwaifo AO, Kamendulis LM, Klaunig JE. Depletion of Kupffer cells modulates ethanol-induced hepatocyte DNA synthesis in C57Bl/6 mice. Environ Toxicol. 2014;29(8):867-75. doi:10.1002/tox.21863
18. Viriyavejakul P, Khachonsaksumet V, Punsawad C. Liver changes in severe *Plasmodium falciparum* malaria: histopathology, apoptosis and nuclear factor kappa B expression. Malar J. 2014;13:106. doi:10.1186/1475-2875-13-106
19. Nguyen-Lefebvre AT, Horuzsko A. Kupffer cell metabolism and function. J Enzym Metab. 2015;1(1):1-26.
20. Sato K, Hall C, Glaser S, Francis H, Meng F, Alpini G. Pathogenesis of Kupffer cells in cholestatic liver injury. Am J Pathol. 2016;186(9):2238-47. doi:10.1016/j.ajpath.2016.06.003
21. Rahima SA, Dewi R, Rumastika NS, Helianti D. Shallot (Allium cepa L.) skin ethanol extract neutralizes liver oxidative stress in diazinon-induced Wistar rats. Qanun Med. 2022;6(1).
22. Cahya N, Dewi R, Hasan M, Helianti D. Ekstrak ethanol kulit bawang merah (Allium cepa L.) memperbaiki kerusakan hati tikus Wistar yang diinduksi diazinon. J Kedokt Kesehat. 2022;9(3):263-70.
23. Dewantoro D, Sulistyaningsih E, Dewi R. Optimization of CIDR1α-PfEMP1 gene transformation in Escherichia coli BL21(DE3) by heat-shock method: stages of malaria vaccine development. JST J Sains Teknol. 2023;12(1).
24. Dewi R, Agung A, Ratnadewi I, Sawitri WD, Rachmania S. Cloning, sequence analysis, and expression of CIDR1α-PfEMP1 from Indonesian *Plasmodium falciparum* isolate. Curr Top Pept Protein Res. 2019;19.
25. Charan J, Kantharia ND. How to calculate sample size in animal studies? J Pharmacol Pharmacother. 2013;4(4):303-6. doi:10.4103/0976-500X.119726
26. Kramer M, Font E. Reducing sample size in experiments with animals: historical controls and related strategies. Biol Rev Camb Philos Soc. 2017;92(1):431-45. doi:10.1111/brv.12237
27. Greenfield EA. Standard immunization of mice, rats, and hamsters. Cold Spring Harb Protoc. 2020;2020(3):pdb.prot100297. doi:10.1101/pdb.prot100297
28. Kagan L. Pharmacokinetic modeling of the subcutaneous absorption of therapeutic proteins. Drug Metab Dispos. 2014;42(11):1890-905. doi:10.1124/dmd.114.059428

29. Rachmania S, Sulistyaningsih E, Ratna Dewi AAI. Recombinant DBL2β-PfEMP1 of the Indonesian *Plasmodium falciparum* induces immune responses in Wistar rats. J Taibah Univ Med Sci. 2021;16(3):422-30. doi:10.1016/j.jtumed.2020.12.017
30. Viola M, Sequeira J, Seiɜa R, Veiga F, Serra J, Santos AC, et al. Subcutaneous delivery of monoclonal antibodies: how do we get there? J Control Release. 2018;286:301-14. doi:10.1016/j.jconrel.2018.08.001
31. Bittner B, Richter W, Schmidt J. Subcutaneous administration of biotherapeutics: an overview of current challenges and opportunities. BioDrugs. 2018;32(5):425-40. doi:10.1007/s40259-018-0295-0
32. Noh ASM, Tan DC, Khir NAM, Shafin N, Ismail CAN. A review on complete Freund's adjuvant-induced arthritic rat model: factors leading to its success. IIUM Med J Malaysia. 2022;21(4):3-12.
33. Ruiz JT, Lujбn L, Blank M, Shoenfeld Y. Adjuvants-and vaccines-induced autoimmunity: animal models. Immunol Res. 2017;65(1):55-65. doi:10.1007/s12026-016-8819-5
34. Taylor BJ, Orr SA, Chapman JL, Fisher DE. Beyond-use dating of extemporaneously compounded ketamine, acepromazine, and xylazine: safety, stability, and efficacy over time. J Am Assoc Lab Anim Sci. 2009;48(6):718-26.
35. Vdoviaková K, Petrovová E, Kre áková L, Maloveská M, Teleky J, Jenčová J, et al. Importance of rat liver morphology and vasculature in surgical research. Med Sci Monit. 2016;22:4716-28. doi:10.12659/MSM.901741
36. Basit H, Tan ML, Webster DR. Histology, Kupffer cell. In: StatPearls [Internet]. Treasure Island (FL): StatPearls Publishing; 2022.
37. Maulina M. Zat-zat yang mempengaruhi histopatologi hepar. 1st ed. Lhokseumawe: UNIMAL Press; 2018.
38. Astitu VER, Muktamiroh H, Harfiani E, Thadeus MS. Gambaran histopatologi hepar mencit yang diinduksi aloksan: perubahan setelah pemberian ekstrak biji hijau kopi Aceh Gayo. Seminar Nasional Riset Kedokteran. 2023.
39. Taber KS. The use of Cronbach's alpha when developing and reporting research instruments in science education. Res Sci Educ. 2018;48(6):1273-96. doi:10.1007/s11165-016-9602-2
40. Singla K, Sandhu SV, Pal RAGK, Bansal H, Bhullar RK, Kaur P. Comparative evaluation of different histoprocessing methods. Int J Health Sci. 2017;11(2):28-34.
41. Bonasia DE, Marmotti A, Massa ADF, Ferro A, Blonna D, Castoldi F, et al. Intra- and inter-observer reliability of ten major histological scoring systems used for the evaluation of in vivo cartilage repair. Knee Surg Sports Traumatol Arthrosc. 2015;23(9):2484-93. doi:10.1007/s00167-014-3024-y
42. Tavakol M, Dennick R. Making sense of Cronbach's alpha. Int J Med Educ. 2011;2:53-5. doi:10.5116/ijme.4dfb.8dfd
43. Jalili C, Farzaei MH, Roshankhah S, Salahshoor MR. Resveratrol attenuates malathion-induced liver damage by reducing oxidative stress. J Lab Physicians. 2019;11(3):212-9. doi:10.4103/JLP.JLP_30_19
44. Adeluwoye AO, Odunola OA, Gbadegesin MA, Adelabu OO. Assessment of the effect of ethanol extract of Tridax procumbens Linn. on sodium arsenite-induced toxicities in male Wistar rats. Am J Biomed Sci. 2017;9(3):151-65.
45. Sari WN, Saebani S, Dhanardhono T. Pengaruh pemberian butylated hydroxytoluene per oral dosis bertingkat terhadap gambaran histopatologis hepar tikus Wistar. J Kedokt Diponegoro. 2018;7(2):1344-57.
46. Ramamoorthy H, Abraham P, Isaac B, Selvakumar D. Mitochondrial pathway of apoptosis and necrosis contribute to tenofovir disoproxil fumarate-induced renal damage in rats. Hum Exp Toxicol. 2019;38(3):288-302. doi:10.1177/0960327118797118
47. Kers J, Leemans JC, Linkermann A. An overview of pathways of regulated necrosis in acute kidney injury. Semin Nephrol. 2016;36(3):139-52. doi:10.1016/j.semnephrol.2016.03.002
48. Rahmah MA, Adrial A, Yenita Y. Gambaran histopatologi ginjal mencit (Mus musculus Balb/c) yang diinfeksi dengan Plasmodium berghei. J Ilmu Kesehat Indones. 2021;2(1):7-16.
49. Cawlfield A, Genito CJ, Beck Z, Bergmann-Leitner ES, Bitzer AA, Soto K, et al. Safety, toxicity and immunogenicity of a malaria vaccine based on the circumsporozoite protein FMP013 with the adjuvant army liposome formulation containing QS21. Vaccine. 2019;37(29):3793-803. doi:10.1016/j.vaccine.2019.05.056
50. Kandeil A, Mostafa A, Hegazy RR, El-Shesheny R, El Taweel A, Gomaa MR, et al. Immunogenicity and safety of an inactivated SARS-CoV-2 vaccine: preclinical studies. Vaccines. 2021;9(3):214. doi:10.3390/vaccines9030214